ANALYSIS OF SIR-B DATA FOR HYDROLOGY AND VEGETATION STUDIES

FINAL REPORT

F.T. Ulaby
M.C. Dobson

March 1990

JPL Contract No: 957191
Contractors Report No: 022574-1-F

ANALYSIS OF SIR-B DATA FOR HYDROLOGY AND VEGETATION STUDIES

FINAL REPORT

F.T. Ulaby
M.C. Dobson

March 1990

JPL Contract No: 957191
Contractors Report No: 022574-1-F

This work was performed for the Jet Propulsion Laboratory, California Institute of Technology, sponsored by the National Aeronautics and Space Administration.

Abstract

Results of experimentation related to the flight of the Shuttle Imaging Radar - B on STS-41G in October, 1984, related airborne L-band SAR and truck-mounted scatterometer are reviewed. The azimuth antenna patterns of SIR-B were successfully measured by an array of receivers. No short term variations in transmit power were observed, but average transmit power was found to be 7 dB below specifications and to vary by 3 dB pass-to-pass. Transfer functions relating SIR-B image digital number to backscattering coefficient were generated on the basis of both arrays of active radar calibrators and distributed target approaches and found to yield equivalent results for several SIR-B passes. The calibrated SIR-B data was shown to be useful in land-use and vegetation cover classification for an agricultural region of Illinois on the basis of image tone and texture. At an incidence angle of 30^{o}, the SIR-B data exhibited a 0.3 dB/.01 g/cm^3 sensitivity to near-surface soil moisture for bare soils and agricultural crops, this is in congruence with prior truck-mounted studies. The magnitude of backscatter recorded by SIR-B is also congruent with levels observed by calibrated scatterometry. Quasi-empirical scattering models are shown to successfully predict the observed SIR-B backscatter from the Illinois region and include terms related to the backscatter from the soil, the volume scatter in the canopy, and interaction of the scattering between the canopy and the soil. The interaction term is shown to dominate for canopies dominated by stalks or trunks (i.e., corn). A model treating the relative polarization phase difference between HH and VV polarizations, is shown to account for the phase differences observed in airborne SAR observations of corn. The model includes terms related to propagation delay through the canopy, forward scatter at the soil surface and bistatic reflection by the stalks. These results are found to be replicated by MIMICS, a first-order vector radiative transfer model for polarimetric backscattering from generalized vegetation canopies. MIMICS is used in sensitivity studies to show a possible technique for unambiguous retrieval of both soil moisture and canopy moisture by taking advantage of the magnitude of both HH- and VV-polarized backscatter and the relative phase difference for a L-band SAR.

Table of Contents

1.0 Overview of Research Project

The research described herein covers a number of specific objectives and tasks as performed over the period from May 1, 1985 until March 31, 1989 by the University of Michigan. This research was initiated in response to RFP No. LC-6-1465 which resulted in JPL Contract No. 957191. An overview of the various research components conducted under this project is given in the following sections.

The activities performed during the SIR-B mission and consequent experimental and analytic efforts can be roughly divided into those dealing with technologic and scientific issues. The technologic issues include evaluation of the SIR-B transmitter and antenna performance, determination of image resolution and definition of an end-to-end system transfer function by reference to external calibration targets. The scientific issues include (1) evaluation of theoretical backscattering models with respect to SIR-B data obtained from soil surfaces and vegetation covered terrain, (2) the correspondence between radar backscatter as measured by truck-mounted scatterometers, airborne SAR and SIR-B, (3) discrimination of natural, within-field variability in σ^o from system related multiplicative noise (fading), (4) evaluation of SIR-B data for monitoring spatial and temporal variations of near-surface soil moisture content, (5) evaluation of SIR-B data for land-use and vegetation classification, and (6) determination of the causative processes for the polarization-phase behavior observed by the JPL L-band SAR for agricultural terrain.

2.0 SIR-B Experiment Data Acquisition

In order to address both the science and technology objectives of this study, a SIR-B test site was established in a relatively flat, agricultural region of west-central Illinois at the intersection point of projected ascending and descending SIR-B coverage. SIR-B, aboard the Challenger on STS-41 G in October 1984, obtained six digital data-takes over the vicinity of this test site from three azimuth view angles

and with local angles of incidence of 17° to 59°. Of the six data-takes, three narrowly missed the prime site due to errors in either the mechanical positioning of the SIR-B antenna and/or the range location of the data window and data-take 38.1 with $\theta = 17°$ was characterized by a poor signal-to-noise ratio. The two ascending data-takes (dt. 49.2 and 97.2) observed the test site during predawn overpasses on October 8 and October 11 respectively both with 30° local angles of incidence but with a 180° difference in azimuth view angle due to the westward drift of the shuttle orbit.

During the OSTA-3 mission, an extensive and intensive set of ancillary data was obtained by field crews, two truck-mounted scatterometers and the JPL L-band airborne SAR mounted on the NASA/Ames CV-990 aircraft. A ground team of approximately 20 individuals operated within an irregularly shaped test area of roughly 20 km x 20 km in size and successfully obtained: (1) truck-mounted scatterometer observations of 50 to 120 agricultural fields per mission day at L-band, (2) a land-use and vegetation canopy survey of over 400 agricultural fields, (3) daily observations of near-surface soil moisture for 100 to 200 agricultural fields per mission day via standard volumetric techniques and via prototype conductance probes designed expressly for this mission, (4) repetitive canopy biomass data for approximately 100 fields, (5) daily precipitation from a 56 gauge network, and (6) measurements of incident power density from SIR-B by five (of six) active radar calibrators (ARCs) which also functioned as transponders for purposes of external calibration.

For a given mission day, the two truck-mounted scatterometers obtained L-band and HH polarized data at the expected local angle of incidence of SIR-B for purposes of external calibration of SIR-B and comparison of measured angular behavior. The land-use and vegetation survey found that the agricultural portion of the test site was comprised of 50% corn fields, 39% soybeans and the remaining 11% devoted to bare soil and various hay crops and pasture. Since the October time period is one of active harvest of corn and soybeans in west-central Illinois, the survey was repeated and it was found that about 10% of the corn fields and 30% of the soybean fields were harvested over the three day period between data-takes 49.2 and

97.2. Harvest operations included removal of harvested biomass, incorporation of remaining biomass into a mulch through plowing or disking and an associated roughening of the soil surface by tillage operations.

An informal network of 56 rain gauges operated by local farmers indicated widespread, but nonuniform, daily rainfalls of 0.2 to 0.5 cm from frontal storms and associated pre-dawn fogs for the period from October 6 through 11. This rainfall yielded in increase in the average soil moisture within the 0-5 cm layer from 0.22 g/cm^3 to 0.3 g/cm^3 over the time period corresponding to data-takes 49.2 and 97.2. The rainfall during the period also contributed to variable moisture conditions in the vegetation canopy where as much as 20% to 30% of the wet mass of soybean and corn foliage can be attributed to rain interception and dew effects.

On each mission day, the JPL L-band airborne SAR flew a series of parallel and offset flight lines over the expected SIR-B image swath. No attempt was made during these flights to provide external calibration for the airborne SAR imagery, and consequently these image are primarily useful in examining the relative phase behavior of the various polarizations.

3.0 SAR Technology Results

The incident power density from the SIR-B SAR was recorded by five L-band ARCs as azimuth cuts of the antenna patterns for each pass. The ARC receivers generally recorded the mainlobe and the second or third sidelobes within the linear portion of the receiver response. The mean beamwidths were found to be $1.1^o \pm 0.04^o$ and $2.4^o \pm 0.05^o$ for the 3 dB and the null-to-null beamwidths respectively. The mean sidelobe levels were found to be -12.0 dB and -10.3 dB for the lead and lag sidelobes respectively. Importantly, the time histories of incident power density recorded by the ARCs exhibit no evidence of pulse-to-pulse variation in SIR-B transmit power over periods of 3 to 5 seconds. All measured patterns are smooth and well-behaved.

The SIR-B antenna pattern in the range direction could not be measured directly by a single ARC, but the pattern may be inferred by comparison of the power density recorded at 5 ARC locations across the SIR-B swath. However, this small sample size is not sufficient to show that the SIR-B range pattern is not that defined by the nominal range pattern. Comparisons of the within-pass time histories of the ARC receivers were used to evaluate the SIR-B antenna boresighting accuracy which was found to vary by $\pm$ 2° from positions estimated from preliminary ephemeris data. Although the transmitter power was found to be stable within a pass, it was found to be 7 dB below specification and to vary by 3 dB pass-to-pass. The range and azimuth spatial resolutions of the SIR-B imagery was examined with respect to the point spread functions generated by the ARCs and found to be nominal.

It is significant to note that the near real-time evaluation of the ARC receiver data in the field permitted a quick assessment of the SIR-B power loss problems as not being located within the antenna corporate feed network.

In order to support the science components of this study, a major effort was placed upon testing external calibration approaches for SIR-B using both point targets and area-extended targets. These approaches were tested for the two data-takes (47.2 and 97.2) which imaged the primary site containing the array of six ARCs and the agricultural fields observed by the two truck-mounted scatterometers. End-to-end system transfer functions relating image digital number to the radar backscatter coefficient σ^o were established independently by the point target and area-extended target approaches. The transfer function takes the form

$$\sigma^o_\theta\,(dB) = 10\ \log\left(\overline{DN^2} - \alpha\right) - \beta_\theta \qquad (1)$$

where α is the mean digital number for image regions expected to represent system noise (ie. shadow areas or specular surfaces) and β is a transfer coefficient dependent upon transmitter power, antenna gains, receiver gain, range and an image scaling coefficient. For both

approaches, α is ascertained from an appropriate portion or the image itself and β is estimated for each specific target (either point target or area-extended target). For data-take 97.2 the six ARCs yield a mean of β = 47.94 dB $\pm$ 1.34 dB while the use of 36 agricultural fields observed by the truck-mounted scatterometer yield a mean of β = 47.86 dB $\pm$ 0.85 dB. Thus, the difference between the two approaches in only 0.1 dB. The larger uncertainty about the mean for the point target approach is related to (1) small sample size, (2) target positioning errors and (3) signal fading of the background. This later factor can be overcome by further increasing the cross-section of the ARC relative to the background.

Pass-to-pass variance in β as calculated by the point target and are-extended target approaches was found to vary in accordance with measured changes in SIR-B transmitter power.

It was concluded that both target approaches are complementary and can yield acceptable calibration transfer functions for both amplitude and phase. The point target approaches are very susceptible to positioning errors and care needs to be taken in proper selection of both target cross section and background conditions. Active point targets were shown by aircraft imagery during the SIR-B overflights and subsequent overflights during the summer of 1985 to have the added advantage of control of polarization; targets can be selected to provide any desired polarization configuration.

4.0 Science Results

4.1 Comparison of Truck-mounted, Airborne and Orbital Backscatter

When the SIR-B SAR imagery is externally calibrated with respect to the point target array of ARCs, $\sigma^o_{SIR\text{-}B}$ is found to be within 1 dB of σ^o_{Truck} for bare soils and agricultural canopies. Linear regression between SIR-B and the truck-mounted scatterometer yields $\sigma^o_{Truck} = 0.96\ \sigma^o_{SIR\text{-}B} - 0.04$ with a linear correlation coefficient r^2

= 0.97. Truck-mounted scatterometer experiments involving tree canopies during the summers of 1986 and 1987 have shown that this equivalence will not hold for trunk-dominated canopies (such as trees) when trunk height exceeds 2m to 3m. For such canopies, a typical truck-mounted system with platform heights on the order of 20m and beamwidths on the order of 4^o to 6^o will become beam limited and not sufficiently sample the ground/trunk interaction terms which can dominate net canopy backscatter. Hence, the use of truck-mounted scatterometry to simulate airborne or orbital SAR response should be confined to short vegetation classes and surfaces.

4.2 Evaluation of SIR-B for Land-Use and Vegetation Classification.

Evaluation of the SIR-B data set for land-use and vegetation classification is somewhat complicated by the fact that the average backscatter from each land-cover category is not time constant, but increases, for example, by an average of 2.5 dB between the two 30^o angle of incidence data-takes separated by three days. This increase can be attributed to both the $0.08 g/cm^3$ increase in soil moisture and associated increases of the water content upon and within the vegetation biomass. The use of multiangle SIR-B data in classification is further complicated by its multi-temporal nature and the fact that active harvest and tillage at this time of year changes the classifications of specific farm fields on a daily basis. However, for single-date (and hence single angle) SIR-B data, image tone alone can be used to readily segment the scene into (1) bright regions consisting of corn, forests and urban areas, (2) moderately bright areas corresponding to harvested corn stubble and rough, plowed fields, (3) moderately dark areas corresponding to harvest ready soybeans, cut soybeans, pasture and hay, and relatively smooth, disked bare soil and (4) water surfaces. The separability between these four general categories is quite good with less than 10% misclassification expected if the scene is filtered to remove the effects of speckle. In addition, textural features can be used to further enhance classification. For example, in the bright target category the magnitude of variance

about the mean and its spatial scale can be used effectively to discriminate urban areas, forests and corn fields.

Multi-temporal data-takes at 30° (d.t. 49.2 and 97.2) can be readily used to discriminate agricultural fields which were either harvested or tilled during the three-day interval. Multi-angle SIR-B data clearly enhances the visual separability of land-use and vegetation classes within each of the four generally categories identified on the basis of tone at a single angle of incidence. Quantitative analysis of the magnitude of this improvement has been frustrated by the lack of overlap of most of the imagery with the 20 km x 20 km prime test site surveyed for land-use and vegetation cover during the mission.

4.3 SIR-B Response to Soil Moisture

Although backscatter at L-band is highly sensitive to near-surface soil moisture, it has been well documented since the mid 1970's that a single polarization L-band SAR is suboptimal for soil moisture classification primarily due to the substantial influence of agronomically induced surface roughness at this wavelength. The HH-polarized SIR-B data substantiates this effect. As a consequence, the scene was subclassified into vegetation cover categories on the basis of tonal stratification into categories of corn, cut corn and rough bare soil (from tillage), short vegetation on a moderately rough soil surface, and short vegetation on a smooth soil surface. The SIR-B sensitivity to soil moisture was evaluated independently for each class using the calibrated data from the two data-takes at a 30° angle of incidence separated by three days. Rainfall over this time period had increased average soil moisture in the 0-5 cm layer by 0.08 g/cm^3. While the magnitude of σ^o is strongly dependent upon the vegetation/surface roughness classification, the time dependency of σ^o for all classes is highly correlated to measured changes in soil moisture. This sensitivity was fond to be approximately the same for all vegetation classes at $\theta = 30^o$ and ranged from 0.26 dB/.01 g/cm^3 to 0.36 dB/.01 g/cm^3 for short vegetation on a smooth soil surface and for corn respectively.

While in this case roughness and vegetation categories could be discriminated on the basis of tonal stratification, this can not be expected to be a generally robust procedure. It is expected that the use of polarimetric and multifrequency SAR data, such as that expected for SIR-C, will greatly enhance the capability to resolve both surface roughness and soil moisture and thereby reduce ambiguities in soil moisture quantification related to surface roughness effects. In addition, it is necessary to classify the vegetation type, since stalk or trunk dominated vegetation covers (such as corn and trees) behave very differently from foliage dominated vegetation covers, and under certain conditions actually enhance the backscatter from the soil due to multiple forward scattering by the ground and the stalks or trunks.

Finally, the latitude of this test site yielded SIR-B trajectories heading at approximately 45° to the cardinal directions. Since farm fields in this area are generally planted and tilled along north/south or east/west directions, no row directional effects were observed in the SIR-B data. This is expected for a SAR look angle at 45° to row direction.

4.4 Radar Scattering Models for Vegetation

Radar scattering models, originally developed on the basis of truck-mounted scatterometer data, were tested using the calibrated SIR-B SAR data to test their adequacy over the range of observed soil roughness, soil moisture, and vegetation biomass conditions quantified at the Illinois test site. A quasi-empirical composite canopy backscatter model consisting of three terms related to (1) volume scatter from the canopy, (2) surface scatter from the soil, and (3) the interaction of surface and volume scatter was initialized for each of the vegetation classes. The model predicts total backscatter as an incoherent sum

$$\sigma^0_{tot} = \sigma^0_{surf} + \sigma^0_{vol} + \sigma^0_{int} \qquad (2)$$

The backscatter from the surface is calculated using the small perturbation approach, which is appropriate for L-band at the

roughness scales encountered, as attenuated by two-way transmission through a canopy of optical depth τ

$$\sigma^o_{surf} = \sigma^o_{soil} \exp(-2\tau \sec\theta) \tag{3}$$

and σ^o_{soil} is determined by the complex permittivity of the soil as estimated empirically on the basis of soil texture and measured soil moisture.

Rayleigh scattering is assumed for the canopy layer which is modeled via an empirical formulation of the "cloud model" as

$$\sigma^o_{vol} = 0.742\ \omega(1 + 0.536\ \omega\tau - 0.237\ (\omega\tau)^2) \times [1 - \exp(-2.119\ \tau \sec\theta)]\cos\theta \tag{4}$$

with the albedo constrained to $\omega = 0.1$ by antecedent studies. The surface/volume interaction term σ^o_{int} is similarly defined by an empirically simplified form which for HH polarization is

$$\sigma^o_{int} = 1.924\ \omega[1 + 0.924\ \omega\tau - 0.398\ (\omega\tau)^2] \times [1 - \exp(-1.925\ \tau \sec\theta)] \times \exp(-1.372\ \tau^{1.12} \sec\theta) \times \exp[-0.836\ (k\sigma^2)\cos\theta]\,|R_{hh}|^2 \cos\theta \tag{5}$$

where $k\sigma$ is a soil surface roughness term and R_{hh} is the Fresnel reflection at the soil surface. This equation applies best to short vegetation canopies not dominated by vertical stalk elements. For corn canopies, a different expression is used

$$\sigma^o_{int} = 2 \exp[-4\ (k\sigma)^2 \cos^2\theta] \exp(-2\tau \sec\theta)\,|R_{hh}|^2\,|R_{st}|^2 \tag{6}$$

where R_{st} is the reflection coefficient of the corn stalks.

The quasi-empirical model yields reasonable fits to SIR-B observations for bare soil cases (zero loss case). Canopy transmission losses and volume scatter are assumed by the model to be caused by canopy elements that are small in size relative to the wavelength and which are assumed to be randomly oriented and distributed disc-shaped elements. The composite canopy model, which included the surface/volume interaction term does a good job of predicting the backscatter observed by SIR-B for the majority of site canopy conditions wherein the canopy elements meet the model assumptions and the optical depth and the albedo are small (i.e., alfalfa, clover and soybeans). However, the model fails to account for the observed level σ^o and soil moisture sensitivity of σ^o for corn canopies unless the modified stalk interaction term is used to account for the multiple forward scatter from the stalks and the soil.

While the inclusion of the simplified formulation given by (6) results in reasonable fits to the corn observations, the dominance of this term as contributing to net backscatter made it imperative to refine the scattering formulation to accurately account for both the amplitude and relative phase effects of vertical stalk and/or trunk components. Model revisions were undertaken to explain the relative phase differences between HH- and VV-polarized airborne SAR data observed at the Illinois site for various canopy conditions including corn and to generalize the model to account for trees wherein Rayleigh region assumptions cannot be used for the trunk components.

4.5 Model Extensions to Account for Stalks/Trunks and the Relative Phase Difference Between HH and VV Backscatter

The under flights of SIR-B by the JPL L-band airborne SAR provided polarimetric imagery of the Illinois test site. In addition to the amplitudes at each of the four linear polarizations, this data was used to calculate the relative phase difference between the HH- and VV- polarized returns and has been defined as the polarization phase

difference $\Delta\phi$ which is obtained from the product of HH and VV signal voltages as

$$V_H V_V^* = A_H A_V e^{j\Delta\phi} \qquad (7)$$

where $\Delta\phi = \phi_H - \Delta_V$. For the Illinois data, the distributions of $\Delta\phi$ for most target classes yield $\overline{\Delta\phi}$ within about 25° and with standard deviations that varied with surface roughness and cover type. Corn canopies yielded a dramatic exception to this general behavior with $\overline{\Delta\phi}$. varying rapidly from about $\overline{\Delta\phi} \approx 20°$ at $\theta < 25°$ to $\overline{\Delta\phi} \approx 140°$ at $\theta < 35°$. A propagation model was developed to explain the polarization phase behavior of these corn canopies most of whose biomass is contained in an array of vertically oriented stalks.

The model treats the canopy as behaving in a fashion similar to a uniaxial crystal characterized by differing velocities of propagation for waves with horizontal and vertical polarizations. The model treats $\overline{\Delta\phi}$ as the summation of polarization dependent propagation delay through the vegetation, forward scatter at the soil surface and specular bistatic reflection by the stalks. The corn canopy is modeled as a two-dimensional array of randomly located vertical cylinders of dimensions and dielectric properties determined by field observations. The plant foliage is ignored since the leaves accounted for only 12% of the biomass and were found to provide a negligible contribution to net backscatter. For a typical corn field, the model predicts that $\overline{\Delta\phi}$ will increase rapidly with incidence angle θ between 25° and 30° due bistatic reflection from the stalks and then $\overline{\Delta\phi}$ decreases gently at $\theta > 30°$ due to differential propagation losses through the canopy. The predictions of canopy propagation losses were confirmed by a series of experiments conducted during the summer of 1986 using a truck-mounted transmitter and rail-mounted receivers to record the transmission properties of corn canopies of various densities. The net phase difference predicted by the model compares very well with the

angular behavior of $\overline{\Delta\phi}$ observed for corn by the airborne SAR at the Illinois test site.

In order to generalize the scattering models to all classes of vegetation including trees and to also incorporate average relative phase relationships into a unified treatment, a first-order vector radiative transfer model was developed. This model was developed during 1987 and 1988 and has come to be known as the Michigan Microwave Canopy Scattering (MIMICS) Model. This model is fully polarimetric and operates over frequencies between 0.5 GH_z and 10 GH_z. It treats the vegetation canopy as consisting of two layers (a crown layer of foliage and branches superimposed over a stalk or trunk layer) located above a dielectric ground surface of variable roughness. The boundaries of the canopy layers are considered to be diffuse and therefor no reflection is considered at the boundaries. Each canopy region is modeled as a random distribution of discrete scatterers characterized by a number density of scattering elements, probability density functions for scatterer size, shape and orientation, and dielectric properties of the scatterers. The trunk region is treated as a random distribution of smooth dielectric cylinders specified by probability density functions for diameter, height, and orientation and also dielectric properties. The first order solution of the vector radiative transfer equation accounts for single scattering within each region of the canopy and double scattering between pairs of regions (i.e., crown/ground and ground/trunk).

The intensity incident upon the canopy is related to the backscattered intensity by a 4x4 transformation matrix. The transformation matrix is dependent upon (1) a reflectivity matrix and a rough surface scattering matrix characterizing specular scattering and backscattering respectively at the soil surface, (2) an extinction matrix for both the crown and trunk layers which specifies attenuation due to absorption and scattering within the layers, and (3) a phase matrix for each canopy layer which specifies the distribution of scattered intensities as averaged over the scatterer size and orientation distributions. The rough surface scattering matrix can be computed using the Kirchoff model with either the stationary phase or

scalar approximations or by the small perturbation approach depending upon the degree of surface roughness relative to wavelength.

The performance of MIMICS has been tested and verified for a number of experimental data sets. MIMICS accurately predicts the angular behavior of $\overline{\Delta\phi}$ observed for corn by the L-band airborne SAR underflights of SIR-B. Experimental observations of a walnut orchard by a polarimetric L-band scatterometer provided diurnal measurements over a two week period. Using the ancillary data measured in the field, MIMICS accurately predicts the observed backscattering behavior as functions of both incidence angle and polarization. Furthermore, it does so on a diurnal basis over the full experimental time period. Another experimental data set acquired by the JPL airborne SAR near Fairbanks, Alaska in March of 1988 has also been used to validate MIMICS. In this effort the externally calibrated SAR image data at L-band has been used to verify the accuracy of MIMICS predictions of polarimetric backscatter from boreal forest stands of white spruce, black spruce, balsam poplar and alder under two radically different environmental conditions: frozen vs. thawed conditions of the tree biomass.

These model validation efforts are particularly significant in that they provide confidence in using MIMICS as a research tool to conduct sensitivity studies. Such studies can lend considerable insight into the formulation of tractable inversion approaches for deriving estimates of selected biophysical quantities such as biomass, canopy water content, and soil moisture.

4.6 Recent Results - Estimation of Soil Moisture Beneath a Stalk or Trunk Dominated Canopy

Of particular interest is the ability to deconvolve the SAR return from terrain in order to estimate both soil moisture and vegetation related quantities such as biomass or canopy water content. The MIMICS Model has been used to investigate the feasibility of using the information provided by a single frequency polarimetric SAR to

retrieve estimates of both soil moisture and canopy water content from a single observation, that is at one angle of incidence. MIMICS sensitivity studies were performed for a stalk-dominated canopy such as corn at L-band. These studies were conducted at both $\theta = 30^o$ and 50^o in order to identify retrieval approaches which would take advantage of both the amplitude and relative phase information to eliminate ambiguities in soil moisture estimation resulting from the presence of the vegetation canopy.

Although both soil moisture and canopy water content are coupled on a seasonal basis due to phenology and on a shorter term basis due to interception of rainfall and dew, they are treated as independent random variates in this sensitivity study. For a corn canopy specified by the number density of stalks and their height and diameter distributions, MIMICS is used to compute the net backscatter as continuous functions of both soil moisture and stalk moisture. Figure 1 shows model calculations for σ^o_{HH}, σ^o_{VV} and $\overline{\Delta\phi}$ at an incidence angle of 30^o. Both σ^o_{HH} and σ^o_{VV} are shown to be relatively insensitive to stalk moisture and primarily sensitive to soil moisture. Conversely, $\overline{\Delta\phi}$ is shown to highly dependent upon stalk moisture and the dependence upon soil moisture is negligible.

This suggests that $\overline{\Delta\phi}$ can be used to estimate stalk moisture and this quantity can then be used in conjunction with either σ^o_{HH} or σ^o_{VV} to provide an estimate of soil moisture. Figure 2 illustrates the insensitivity of $\overline{\Delta\phi}$ to soil moisture and the covariance of σ^o_{HH} and σ^o_{VV} to both soil and stalk moisture. An example of how this may be used to provide unambiguous estimates of soil moisture is given by Figure 3. Dry stalk conditions (i.e., stalk moisture = 0.32) yields $\overline{\Delta\phi} = -44^o$ as shown in Figure 3a. Contours of constant σ^o_{HH} and σ^o_{VV} are shown to both intersect the $\overline{\Delta\phi} = -44^o$ line at a soil moisture of 0.14 g/cm^3. For wet stalk conditions wherein stalk moisture is 0.7 as shown in Figure 3b, the contours of constant σ^o also intersect at a unique triple-point specifying both soil and stalk moisture. Using MIMICS at $\theta = 30^o$, it can be shown that any combination of stalk and soil moisture yields a

unique triple-point solution for unambiguous retrieval of both quantities. On the basis of the $\theta = 30^o$ simulations alone, it can be argued that this result could also be achieved on the basis of the intersection point of any two of the three pieces of SAR information σ^o_{HH}, σ^o_{VV} or $\overline{\Delta\phi}$ However, such a two-parameter approach is not robust at all angles of incidence.

The MIMICS simulations for the same corn canopy are shown in Figure 4 at $\theta = 50^o$. In a fashion similar to that obtained at $\theta = 30^o$, both σ^o_{HH} and σ^o_{VV} are sensitive to soil moisture and σ^o_{VV} more so than σ^o_{HH}; however the sensitivity of σ^o_{VV} to stalk moisture is much greater than determined at $\theta = 30^o$. In addition, there is no longer a nearly linear dependence of $\overline{\Delta\phi}$ upon stalk moisture at $\theta = 50^o$; $\overline{\Delta\phi}$ is shown in Figure 4 to be ambiguous with respect to stalk moisture. Contours of constant σ^o and $\overline{\Delta\phi}$ are shown in Figure 5 for the 50^o case. The solution spaces for 50^o L-band backscatter and $\overline{\Delta\phi}$ for dry and wet conditions are shown in Figure 6. It is readily apparent that the use of σ^o_{HH} and σ^o_{VV} in a two-parameter solution will yield ambiguities for both the wet and dry examples shown. The use of σ^o_{HH} and $\overline{\Delta\phi}$ alone can also lead to ambiguities in the dry case. However, the model consistently predicts that a 3-parameter solution will converge on a unique solution for soil and stalk moisture.

While the component parts of the MIMICS model have been validated versus various sets of empirical data, there is, at present, no data set with which to test the hypothesized approach. We expect to collect such a data set for model validation over the next year.

5.0 Presentations and Publications

5.1 Presented at Symposia and Meetings

[1] Ulaby, F.T.. D.N. Held, and M.C. Dobson, "Vegetation Canopy Discrimination and Biomass Assessment Using Multipolarized Airborne SAR," NASA/JPL Aircraft Radar Workshop, February 4-5, 1985, Jet Propulsion Laboratory, Pasadena, CA.

[2] Dobson, M.C., K. Barkeshli, F.T. Ulaby, and D.R. Brunfeldt, "A Microwave Dielectric Probe for In-Situ Measurement of Volumetric Soil Moisture," 4th International Symposium on Remote Sensing for Soil Survey, March 4-8, 1985, Enschede, The Netherlands.

[3] Dobson, M.C., F.T. Ulaby, and J. Cihlar, "Preliminary Results from the Illinois and Canadian SIR-B Sites," SIR-B Science Team Workshop, May 13-15, 1985, Jet Propulsion Laboratory, Pasadena, CA.

[4] Dobson, M.C., F.T. Ulaby and D.N. Held, "External Calibration of SIR-B Imagery with Area-Extended and Point Targets," 1985 International Geoscience and Remote Sensing Symposium (OGARSS '85)., October 7-9, 1985, Amherst, MA.

[5] Ulaby, F.T., M.C. Dobson, and D.N. Held, "SAR Polarization-Phase of Bare and Vegetated Targets," 1985 International Geoscience and Remote Sensing Symposium (IGARSS '85), October 7-9, 1985, Amherst, MA.

[6] Dobson, M.C., and F.T. Ulaby, "Preliminary Evaluation of the SIR-B Response to Soil Moisture, Surface Roughness, and Crop Canopy Cover," 1985 International Geoscience and Remote Sensing Symposium (IGARSS '85), October 7-9, 1985, Amherst, MA.

[7] Ulaby, F.T., F. Kouyate and L. Williams, "Textural Information in SAR Images," International Geoscience and Remote Sensing Symposium (IGARSS '85), October 709, 1985, Amherst, MA.

[8] Ulaby, F.T. and M.C. Dobson, "SIR-B Measurements and Modeling of Vegetation," 1986 Spaceborne SAR Symposium, April 28-30, 1986, Jet Propulsion Laboratory, Pasadena, CA.

[9] Ulaby, F.T., A. Tavakoli, and M.C. Dobson, "Amplitude and Phase Properties of the Propagation Constant of Vegetation," 1986 International Geoscience and Remote Sensing Symposium (IGARSS '86), September 8-11, 1986, Zurich, Switzerland.

[10] Ulaby, F. T., "Fundamentals of Radar Reflectance from Forest Canopies: A Tutorial," ASPRS/ACSM Convention, Satellite Radar for Assessing Forest Cover, Baltimore, MD, 1 April 1987.

[11] M. C. Dobson, and F. T. Ulaby, "Magnitude Calibration of Polarimetric Airborne SAR at L-Band," IEEE International Geoscience and Remote Sensing Symposium (IGARSS '87), Ann Arbor, Michigan, 18-21 May 1987.

[12] Ulaby, F. T., K. McDonald, K. Sarabandi, and M. C. Dobson, "Michigan Microwave Canopy Scattering Model (MIMICS)," International Geoscience and Remote Sensing Symposium (IGARSS '88). Edinburgh, Scotland, September, 1988.

[13] McDonald, K., M.C. Dobson, and F.T. Ulaby, "Determination of Soil Moisture Beneath a Stalk or Trunk Dominated Canopy by Radar," International Geoscience and Remote Sensing Symposium (IGARSS '88), Edinburgh, Scotland, September, 1988.

[14] DeRoo, R., F.T. Ulaby, Y. Kuga, and M.C. Dobson, "Experimental Studies of the Microwave Backscattering by Well Characterized Surfaces," Progress in Electromagnetics Research Symposium (PIERS), MIT, Cambridge, Massachusetts, July, 1989.

5.2 Publications

[1] Ulaby, F.T., M.C. Dobson, and D.N. Held, "Vegetation Canopy Discrimination and Biomass Assessment Using Multipolarized Airborne SAR," NASA/JPL Aircraft SAR Workshop Proceedings, February 4-5, 1985, JPL Pub. 85-39, June 1985.

[2] Ulaby, F. T., F. Kouyate, B. Brisco and T. H. L. Williams, "Textural Information in SAR Images," IEEE Trans. Geoscience and Remote Sensing, V. GE-24, No. 2, pp. 235-245, 1986.

[3] Dobson, M. C., F. T. Ulaby, D. R. Brunfeldt, and D. N. Held, "External Calibration of SIR-B Imagery with Area-Extended and Point Targets," IEEE Transactions on Geoscience and Remote Sensing, V. GE-24, No. 4, pp. 453-461, 1986.

[4] Dobson, M. C., and F. T. Ulaby, "Preliminary Evaluation of the SIR-B Response to Soil Moisture, Surface Roughness, and Crop

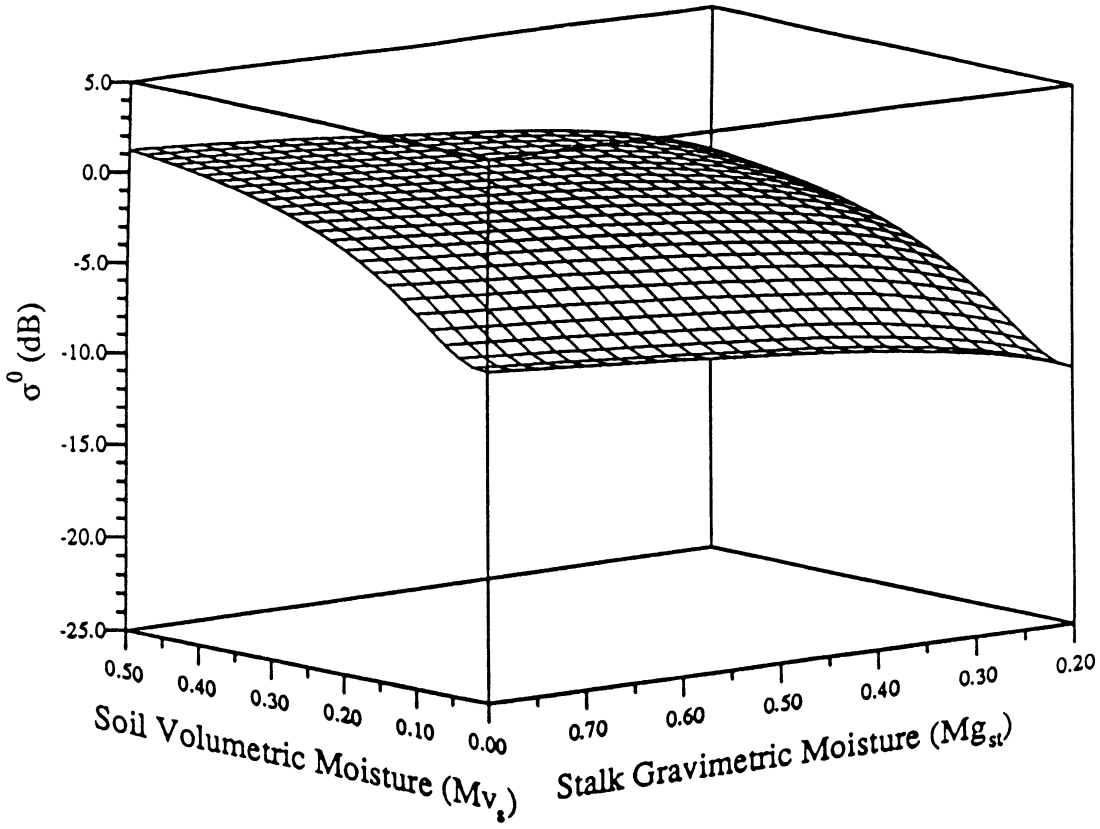

Canopy Backscatter, $\theta=30^{o}$, VV Pol.

Figure 1(b)

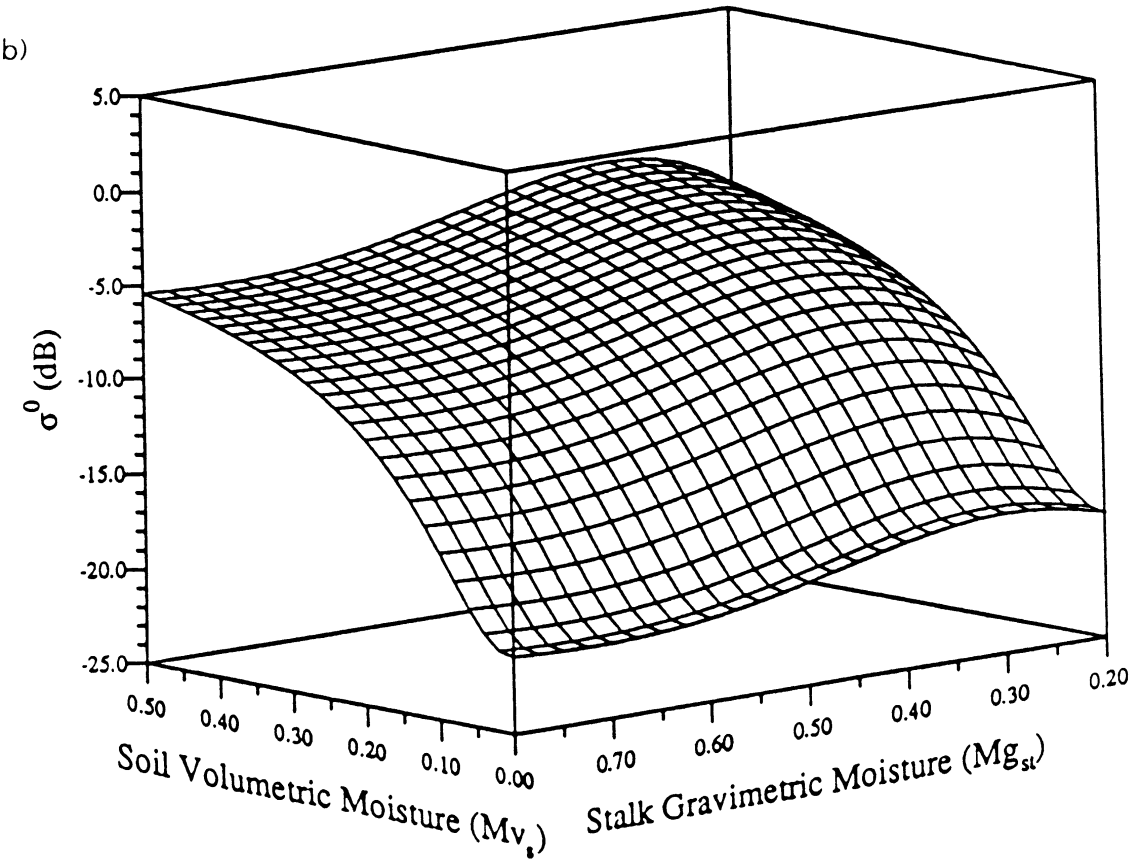

Figure 1. Mimics predicted sensitivity of L-band backscatter at 30^{o} to soil moisture and corn stalk moisture for (a) σ^{o}_{HH} and (b) σ^{o}_{VV}

(c) $\overline{\Delta\phi}$

Canopy Cover," IEEE Transactions on Geoscience and Remote Sensing, V. GE-24, No. 4, pp. 517-526, 1986.

[5] Ulaby, F.T., and M.C. Dobson, "SIR-B Measurements and Modeling of Vegetation," The Second Spaceborne Imaging Radar Symposium, April 28-30, 1986, JPL publication 86-26, pp. 191-200, Dec. 1, 1986.

[6] Ulaby, F. T., D. Held, M. C. Dobson, K. McDonald, and T. B. A. Senior, "Relating Polarization Phase Difference of SAR Signals to Scene Properties," IEEE Trans. on Geoscience and Remote Sensing, V. GE-25, No. 1, 1987, pp. 83-92.

[7] Ulaby, F. T., A. Tavakoli, and M. C. Dobson, "Amplitude and Phase Properties of the Propagation Constant of Vegetation," IEEE International Geoscience and Remote Sensing Symposium (IGARSS '86) Digest, Zurich, Switzerland, 8-11 September 1986.

[8] Dobson, M.C. and F.T. Ulaby, "Magnitude Calibration of Polarimetric Airborne SAR at L-band," International Geoscience and Remote Sensing Symposium (IGARSS '87) Digest, Ann Arbor, Michigan, Vol. 1, p. 527, 18-21 May 1987.

[9] Ulaby, F.T., A. Tavakoli, and T.B.A. Senior, "Microwave Propagation Constant for a Vegetation Canopy with Vertical Stalks," IEEE Transactions on Geoscience and Remote Sensing V. GE-25, No. 6, pp. 714-725, 1987.

[10] Ulaby, F. T., K. McDonald, K. Sarabandi, and M. C. Dobson, "Michigan Microwave Canopy Scattering Model (MIMICS)," accepted for publication by International Journal of Remote Sensing, 1990.

Figure 1(c)

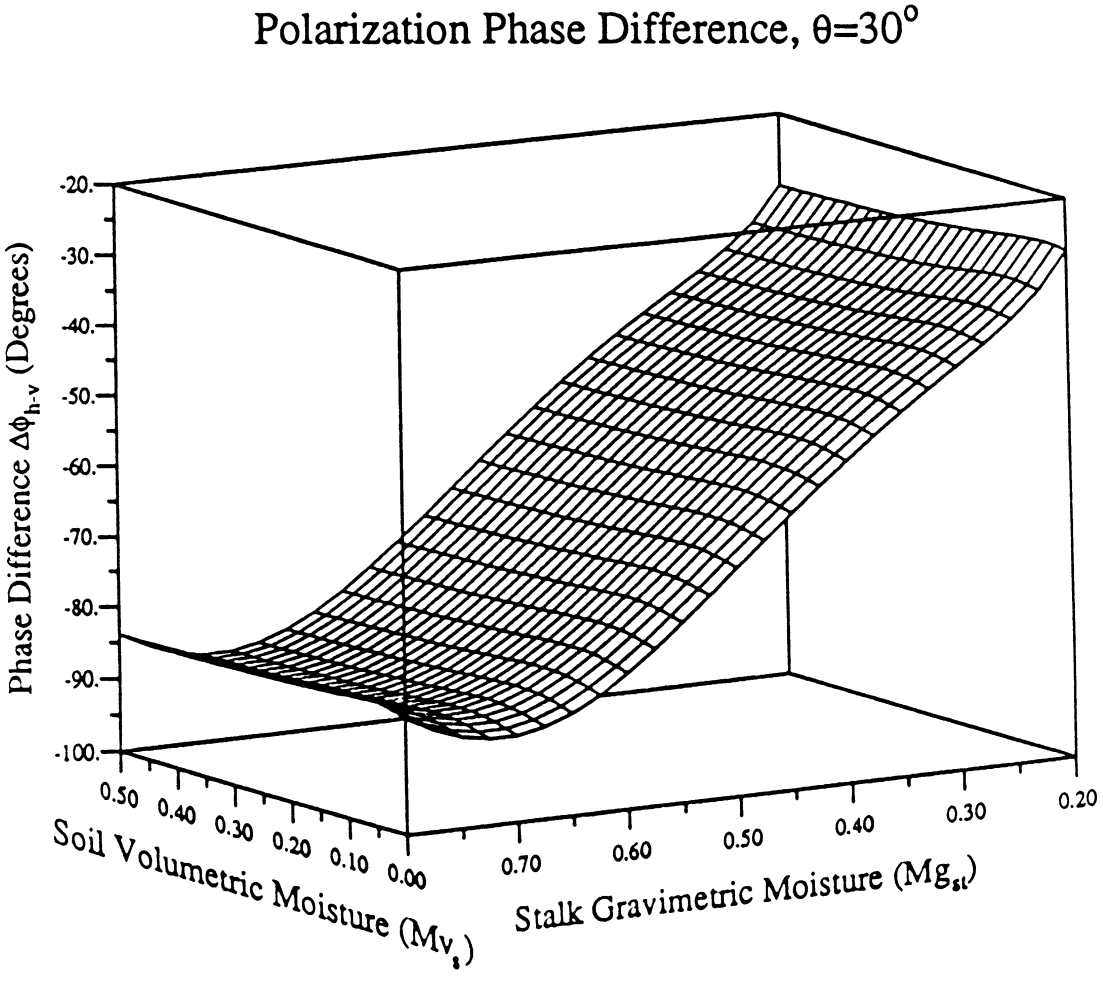
Polarization Phase Difference, θ=30°
Phase Difference Δφh-v (Degrees)
-20.
-30.
-40.
-50.
-60.
-70.
-80.
-90.
-100.
0.50
0.40
0.30
0.20
0.10
0.00
Soil Volumetric Moisture (Mvs)
0.70
0.60
0.50
0.40
0.30
0.20
Stalk Gravimetric Moisture (Mgst)

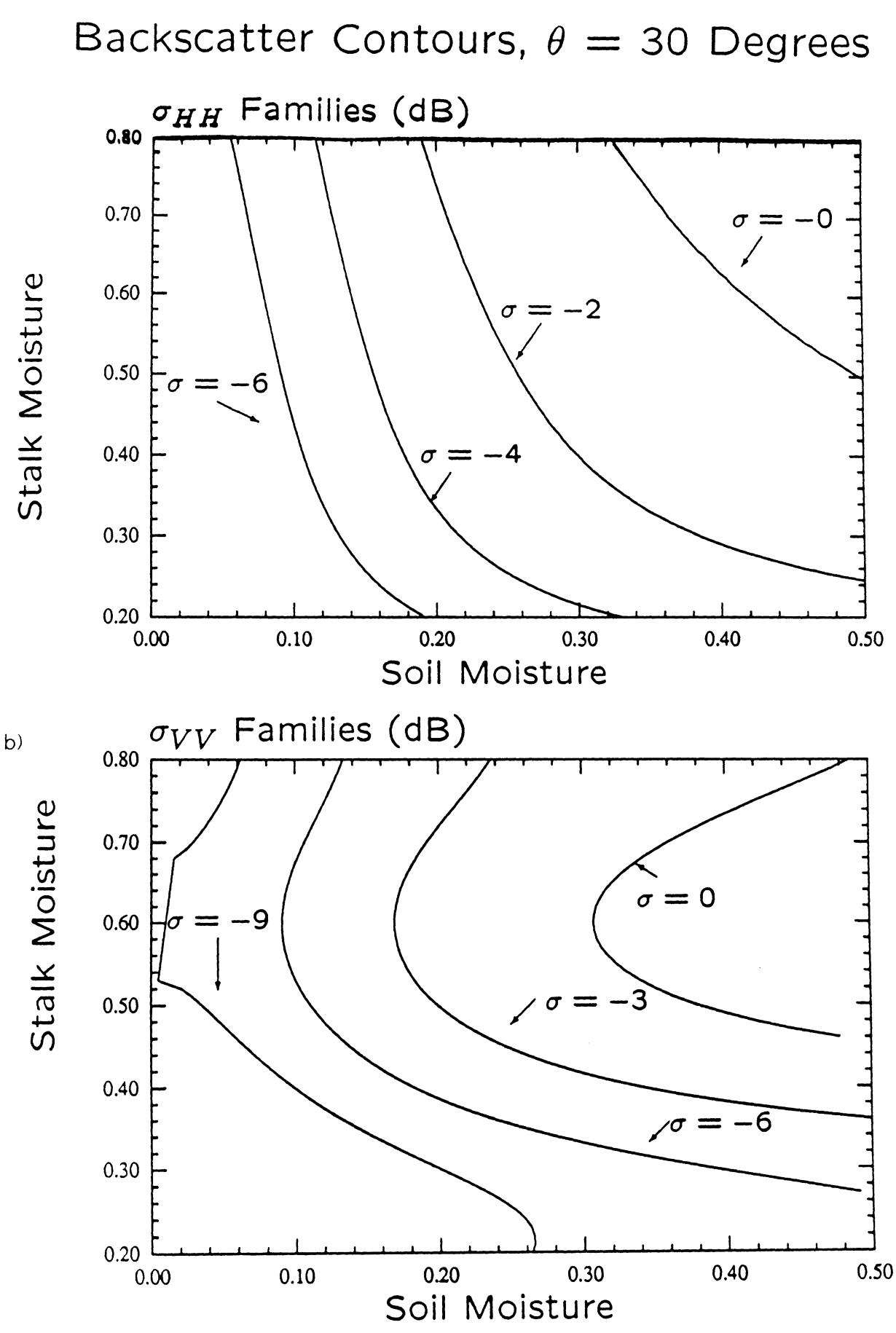

Figure 2. MIMICS derived contours of constant backscatter from corn for L-band at 30° incidence for (a) HH-polarization, (b) VV-polarization and (c) $\overline{\Delta\phi}$

Figure 3(a)

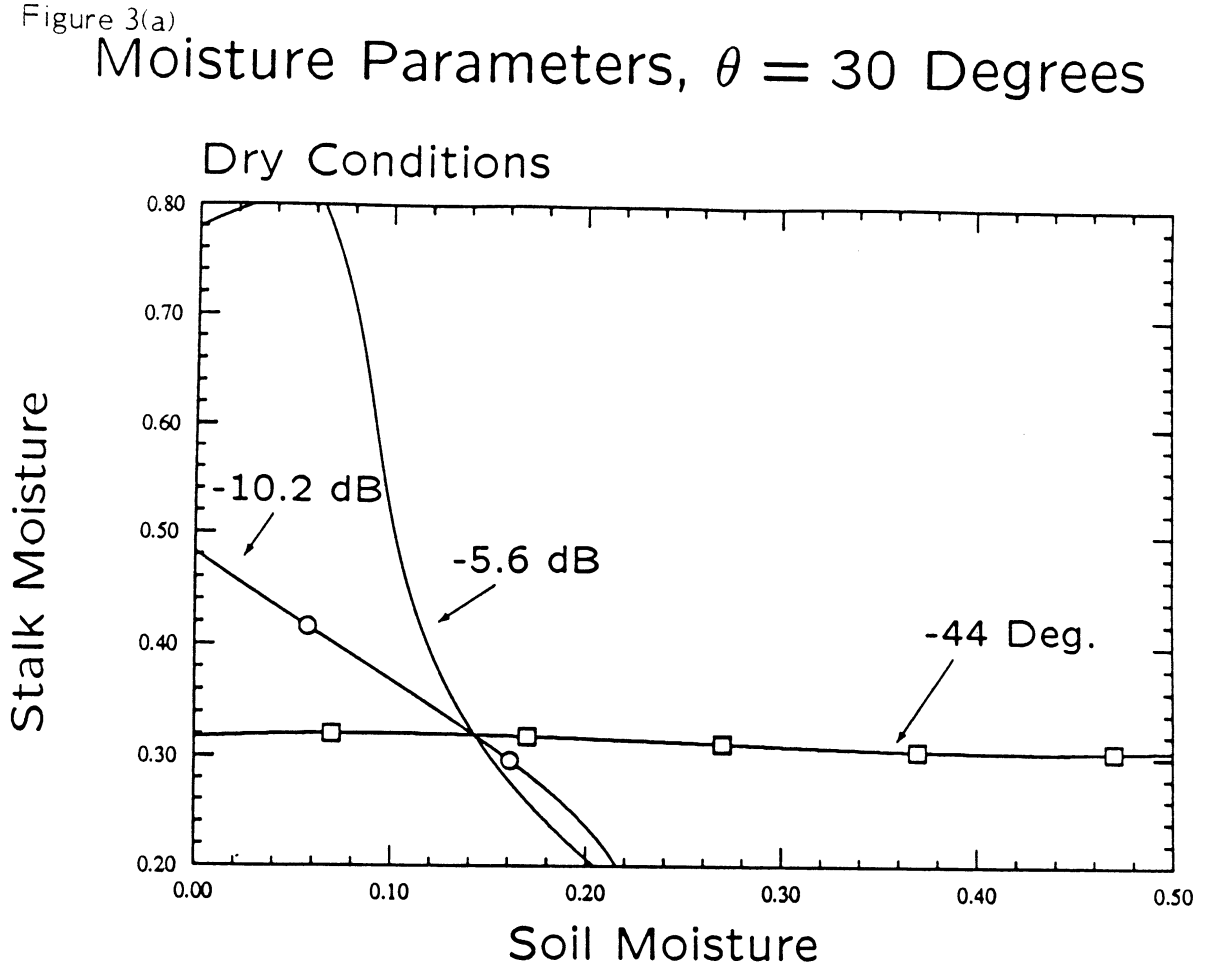

Figure 3(b)

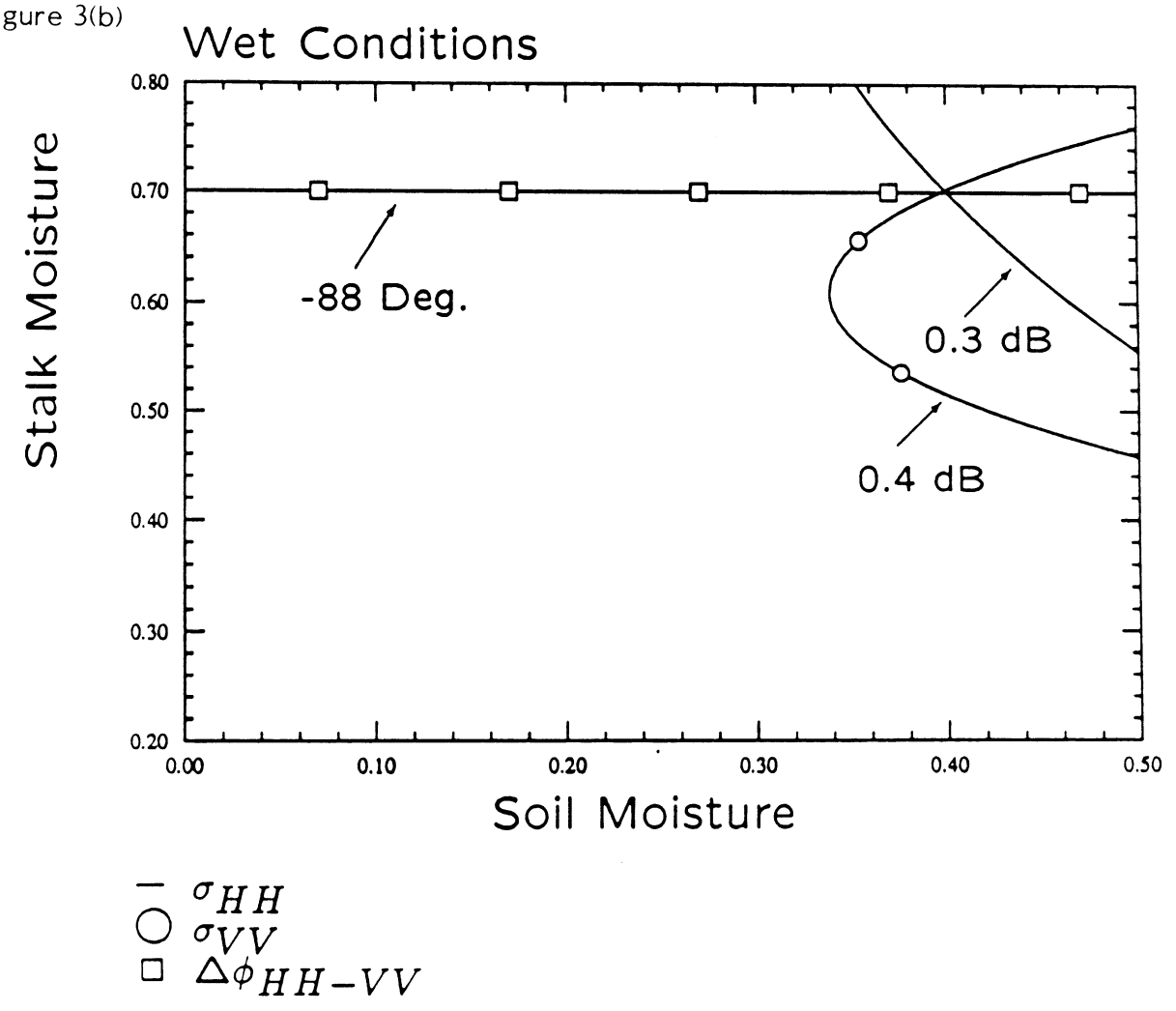

— σ_{HH}
○ σ_{VV}
□ $\Delta\phi_{HH-VV}$

Figure 3. MIMICS predictions of solution space for estimation of both soil moisture and stalk moisture for L-band 30° incidence data for (a) dry conditions and (b) wet conditions.

Figure 4(a)

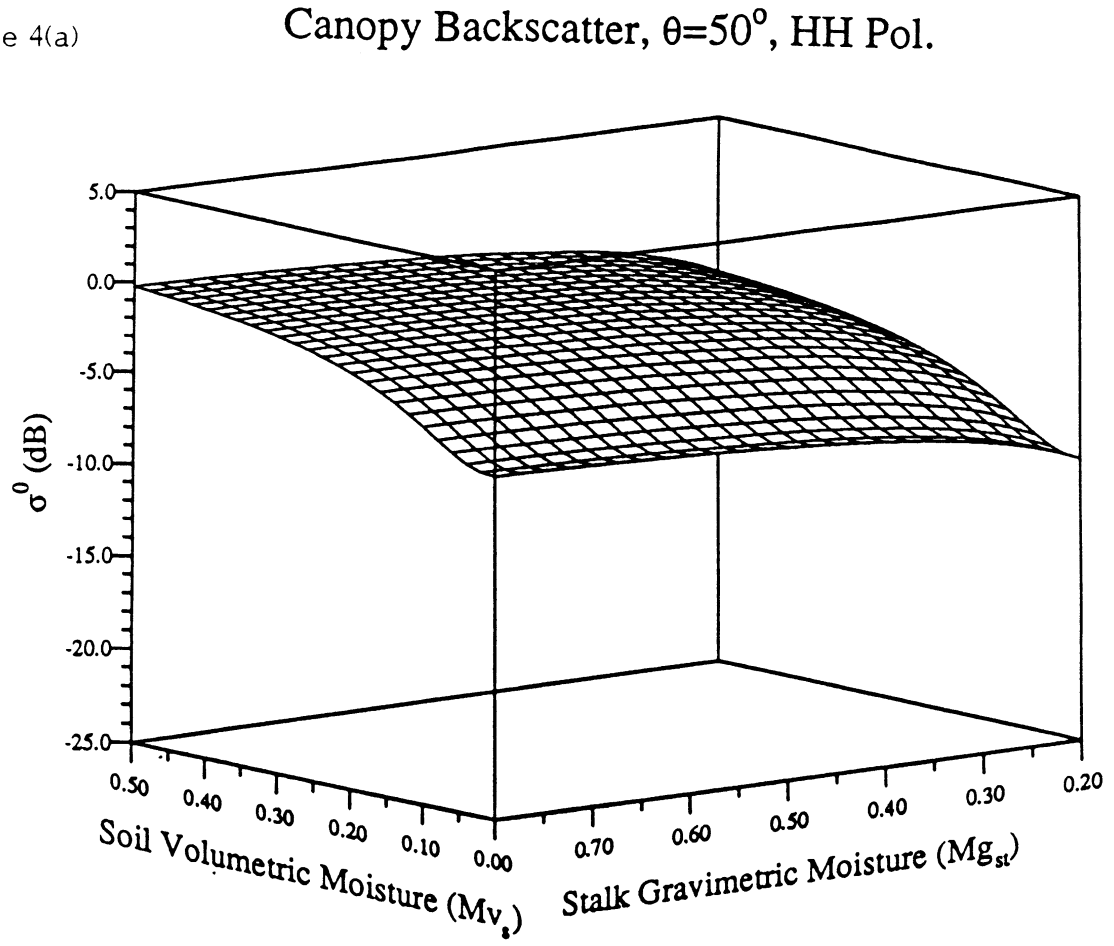

Figure 4(b)

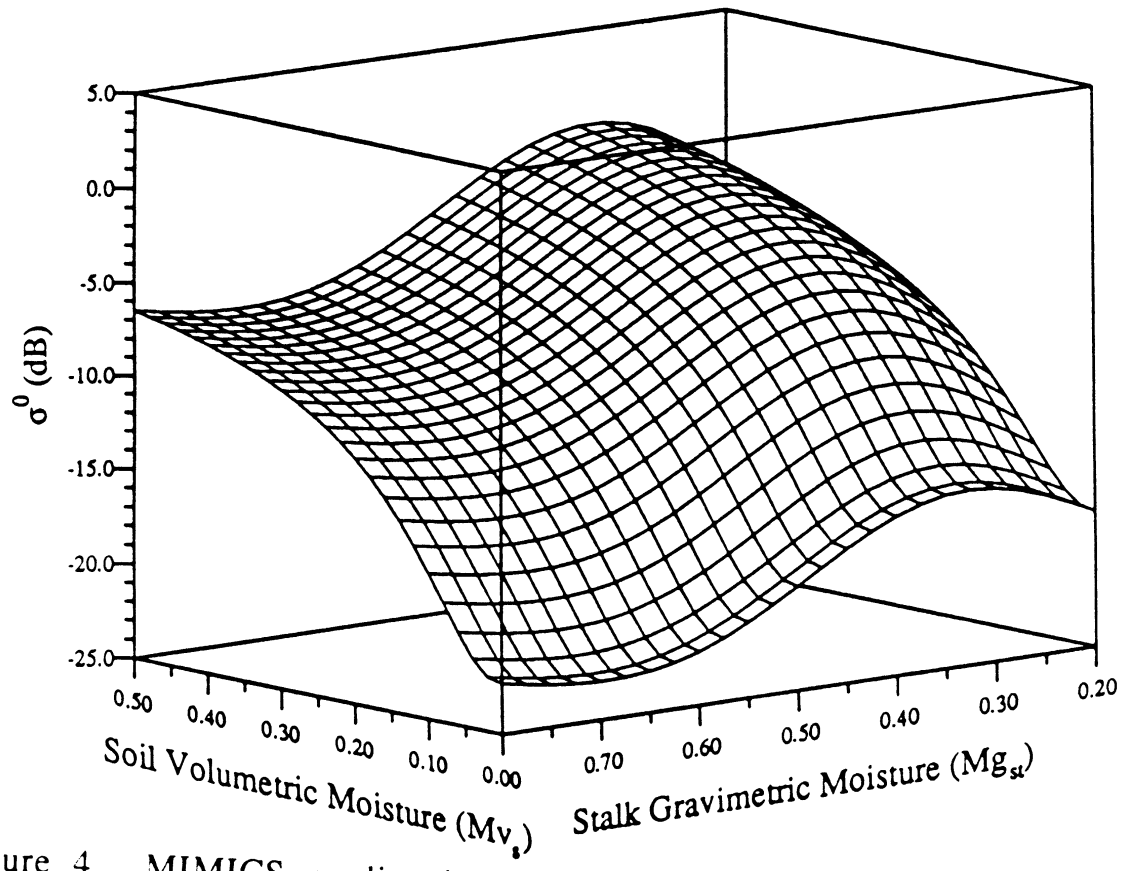

Figure 4. MIMICS predicted sensitivity of L-band backscatter at 50° to soil moisture and corn stalk moisture for (a) σ^{o}_{HH} and (b) σ^{o}_{VV} (c) $\overline{\Delta\phi}$

Figure 4(c)

Polarization Phase Difference, θ=50°

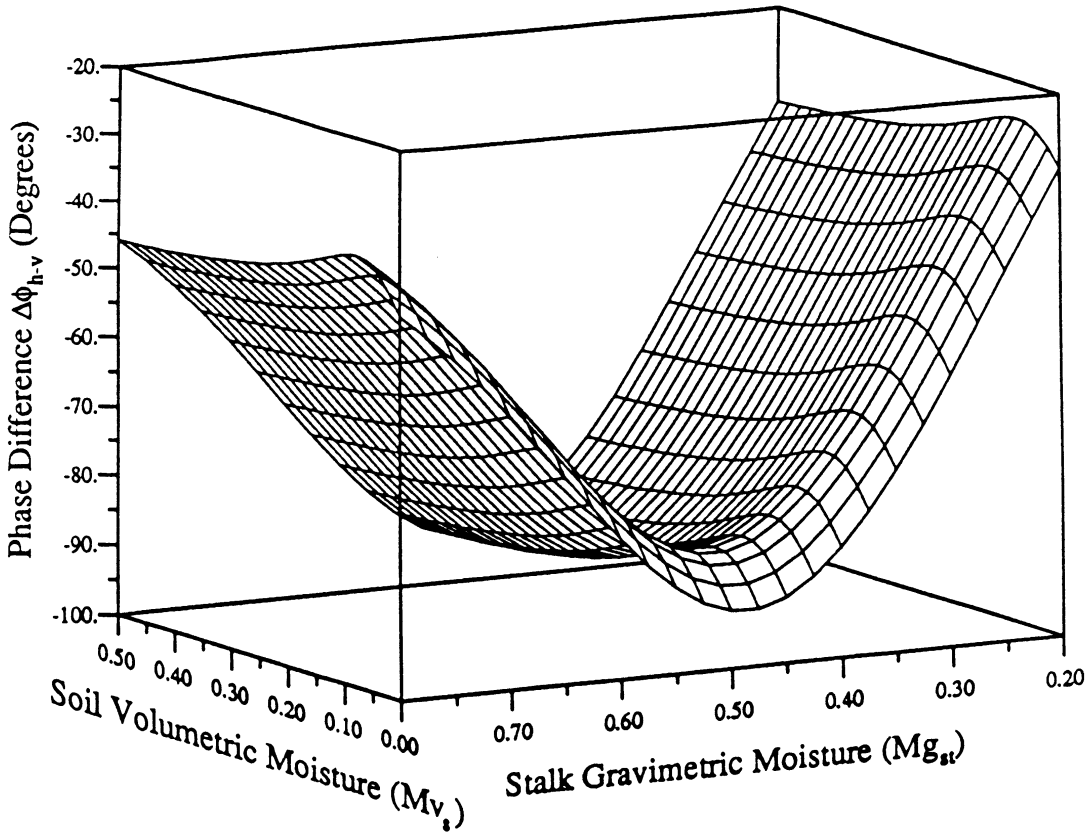

Figure 5(a)

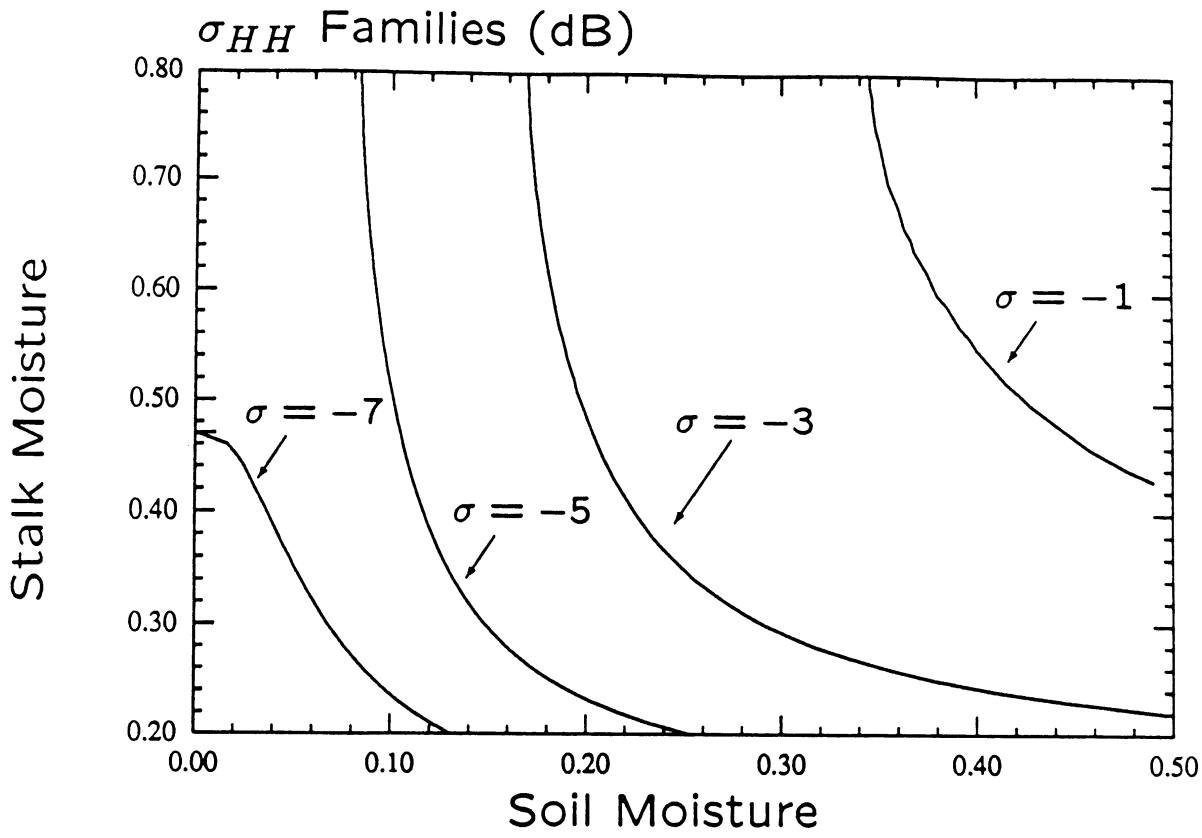

Figure 5(b)

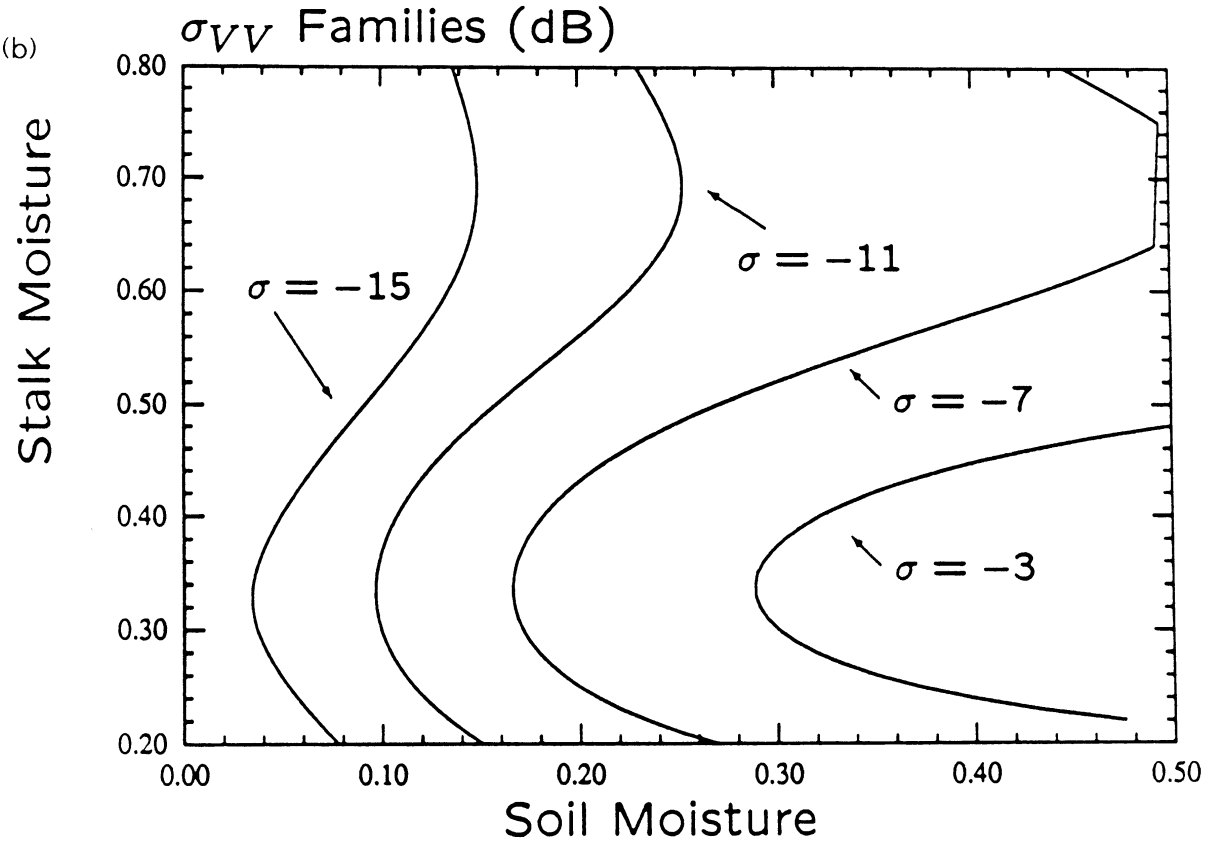

Figure 5. MIMICS derived contours of constant backscatter from corn for L-band at 50° incidence for (a) σ^{o}_{HH} and (b) σ^{o}_{VV} (c) $\overline{\Delta\phi}$

Figure 5(c)

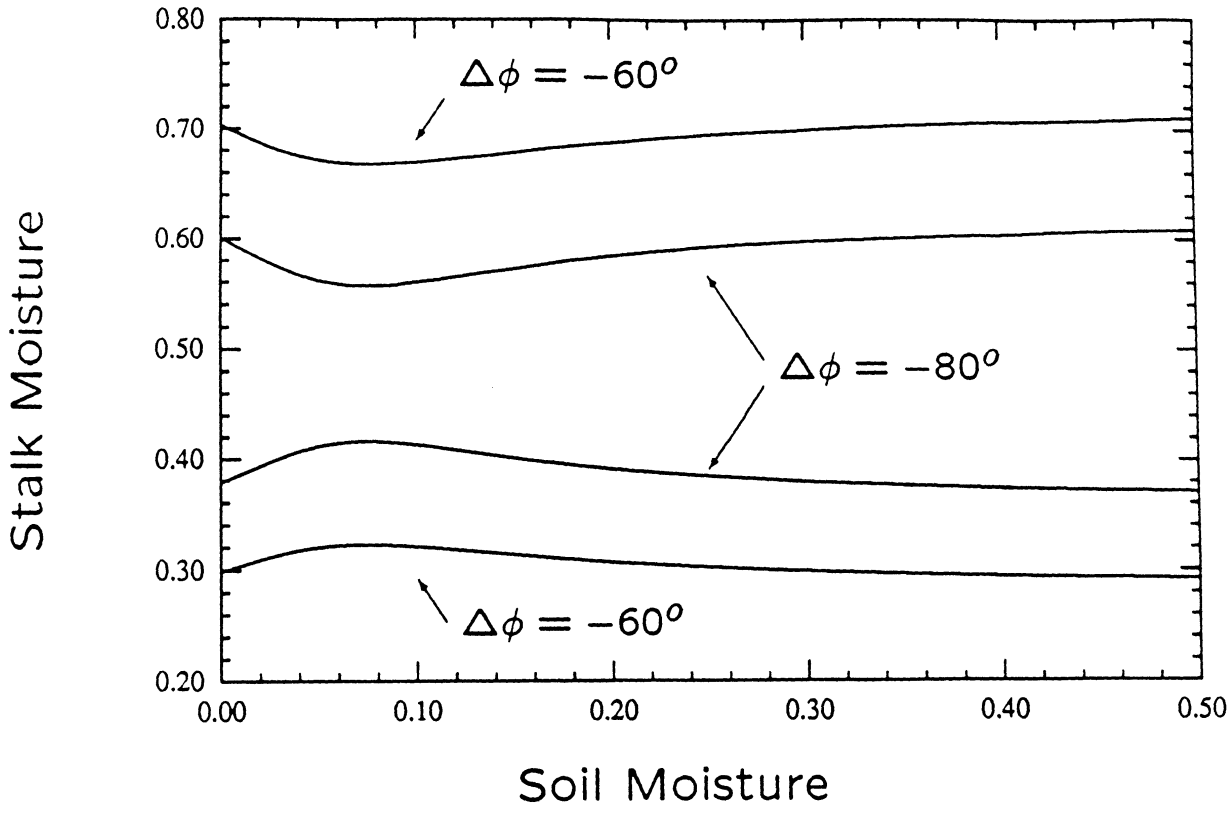
Phase Difference Contours, θ = 50 Degrees
Stalk Moisture
Soil Moisture
0.80
0.70
0.60
0.50
0.40
0.30
0.20
0.00
0.10
0.20
0.30
0.40
0.50
Δφ = −60°
Δφ = −80°
Δφ = −60°

igure 6(a)

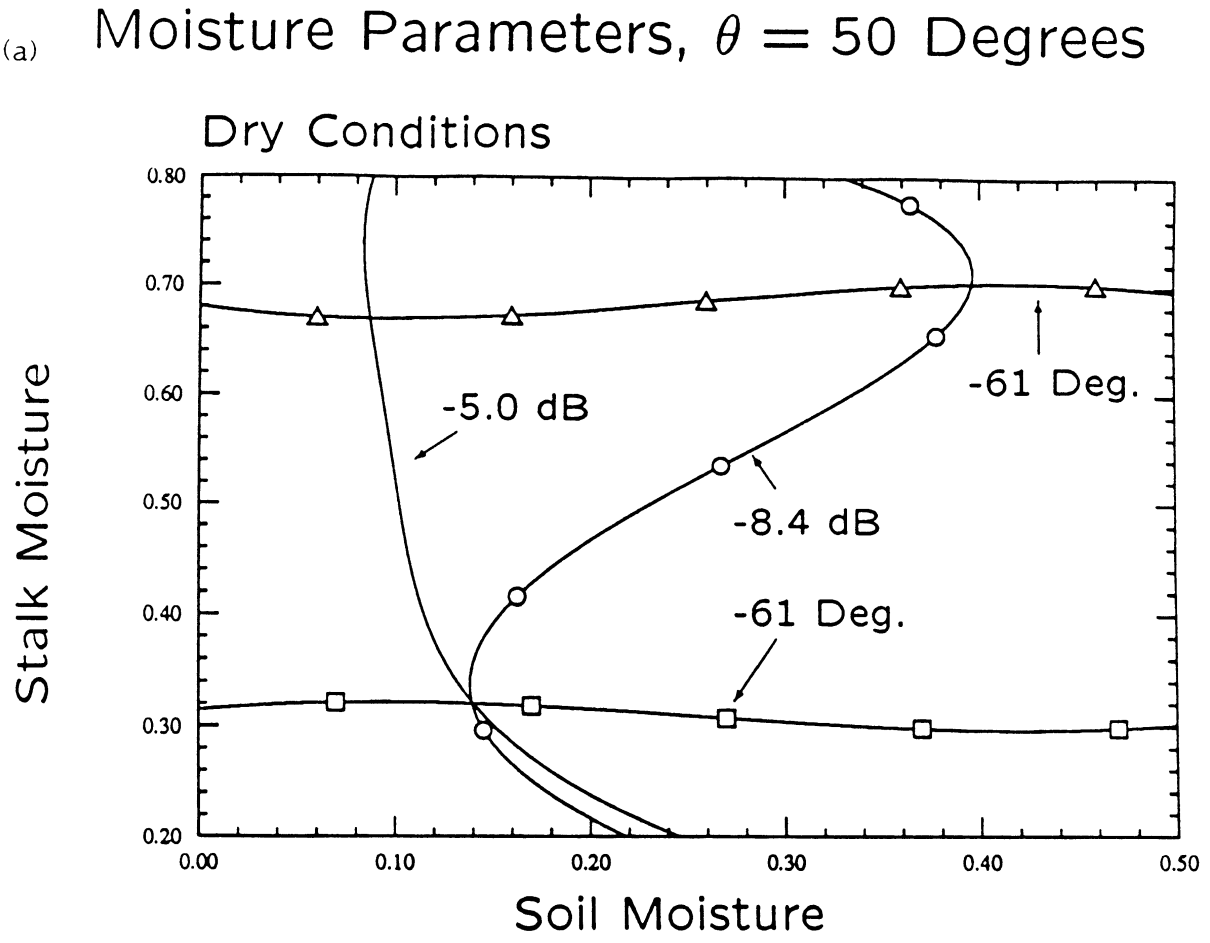

igure 6(b)

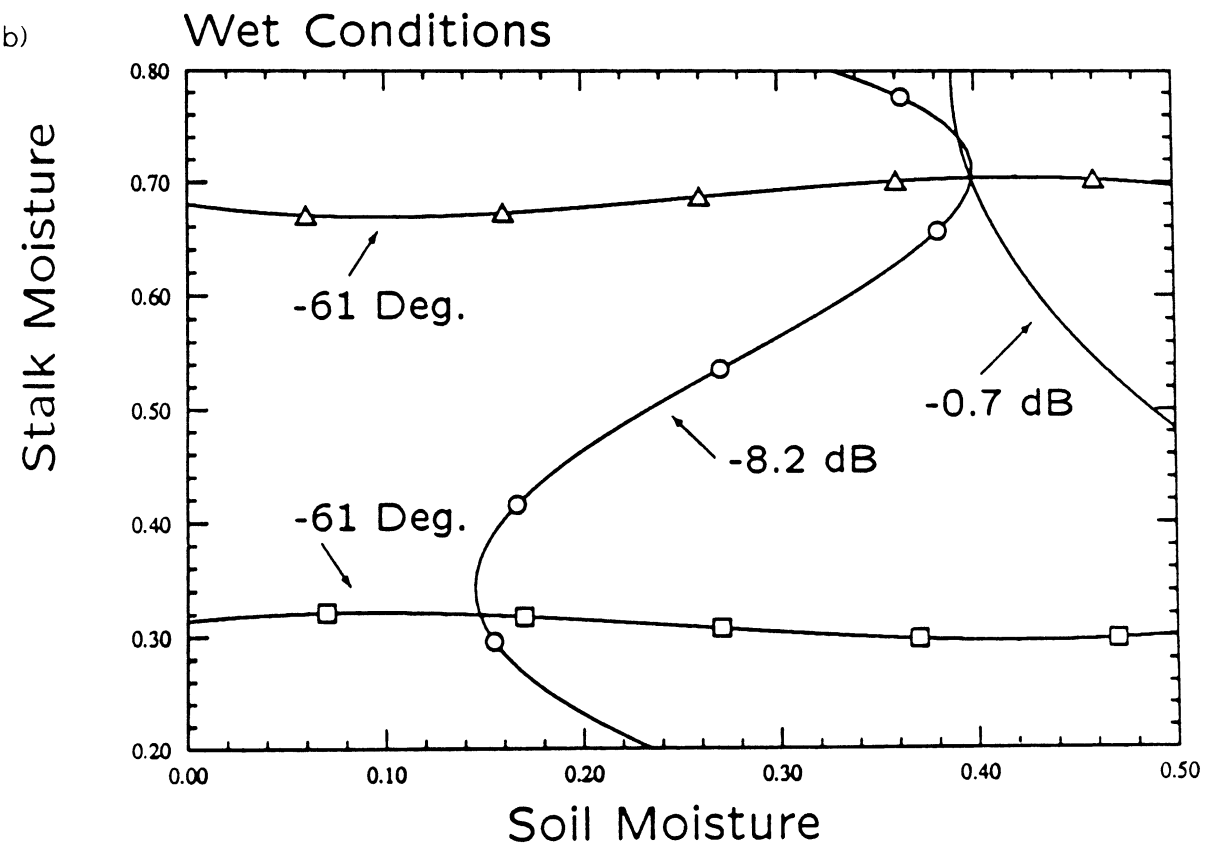

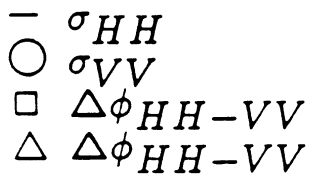

Figure 6. MIMICS predictions of solution space for estimation of both soil moisture and stalk moisture for L-band data at 50° incidence for (a) dry conditions and (b) wet conditions.